Photoluminescence from InN Nanorod Arrays with a Critical Size

2013 Appl. Phys. Express 6 062103

(http://iopscience.iop.org/1882-0786/6/6/062103)

Applied Physics Express **6** (2013) 062103
http://dx.doi.org/**10.7567/APEX.6.062103**

Photoluminescence from InN Nanorod Arrays with a Critical Size

Hyeyoung Ahn[1]*, Yu-Sheng Liu[1], Ke-Yang Chang[1], and Shangjr Gwo[2]

[1]*Department of Photonics and Institute of Electro-Optical Engineering, National Chiao Tung University, Hsinchu 30010, Taiwan*
[2]*Department of Physics, National Tsing Hua University, Hsinchu 30013, Taiwan*
E-mail: hyahn@mail.nctu.edu.tw

Received February 22, 2013; accepted May 16, 2013; published online June 5, 2013

In this report, we investigated the rod size dependence of photoluminescence (PL) from vertically aligned indium nitride (InN) nanorod arrays grown on Si(111) substrates. Abnormal temperature dependence of the PL peak energy and the PL bandwidth was observed for InN nanorods with a critical diameter, which is of the same order of the surface electron accumulation layer (~20 nm). Exceptionally large activation energy of the nanorods with the critical diameter implies that holes within these narrow nanorods need to surpass the band bending energy near the surface in order to recombine with electrons accumulated in the surface layer. © 2013 The Japan Society of Applied Physics

Indium nitride (InN) with a narrow direct band gap has superior electronic transport properties compared with other group-III nitrides so that InN has become attractive for various applications such as high-frequency electronic devices, near-infrared optoelectronics, and high-efficiency solar cells. In order to meet the request of the rapid downsizing of electronic and photonic device dimensions, one-dimensional (1D) InN nanomaterials in the forms of nanowires (NWs), nanorods (NRs), and nanotubes (NTs) have been developed.[1–6] The high surface-to-volume ratio of 1D InN nanomaterials has also been proved to be beneficial for the enhancement of terahertz (THz) wave emission.[7] Several studies reported the results of photoluminescence (PL) from InN films and InN nanostructures.[8–12] Despite superior structural advantages, the observed PL from 1D InN is typically much weaker and its bandwidth is broader than that from the InN epilayer, and its PL mechanism critically depends on the size of nanomaterials.

In this work, we report on the size dependence of the thermal evolution of PL properties for vertically self-aligned InN NRs grown along the wurtzite *c*-axis on Si(111). The temperature dependences of the PL peak energy and PL bandwidth of InN NRs are different from that of the epilayer. In particular, for NRs with the average rod diameter (d) similar to the depth of the surface electron accumulation layer ($2t_s \sim 20$ nm),[13] the radiative recombination of electrons and holes was not sensitive to the increase of temperature up to 60–70 K, and with the further increase of temperature, the PL quenches drastically due to the nonradiative recombination. The estimated activation energy for NRs with the critical diameter ($d \sim 2t_s$) is much larger than that for NRs with $d > 2t_s$, and this large activation energy is of the same order of the downward surface band bending barrier (V_B) for *c*-InN.

For this study, we prepared four InN NR samples with different average rod diameters: sample A ($d = 143/75$ nm), sample B ($d = 33$ nm), sample C ($d = 24$ nm), and sample D ($d = 27$ nm). In sample A, most of the surface area of the film is covered by large-size NRs with $d \sim 143$ nm and a smaller number of NRs with $d \sim 75$ nm fill the gap between large NRs.[14] Samples C and D were chosen to show the characteristic PL response of NRs with $d \sim 2t_s$. Vertically aligned InN NR arrays were grown on Si(111) substrates by plasma-assisted molecular-beam epitaxy (PAMBE) at a sample temperature of 520 °C, and the rod density and diameter were controlled by means of the N/In ratio and the growth time. To obtain the desired columnar morphology, the epitaxial growth proceeded under N-rich conditions, for example, N/In ratios of samples B and C are 4.9 and 4.4, respectively. A 1.2-μm-thick InN epilayer was also prepared for comparison. The details of the growth method and conditions are described elsewhere.[9]

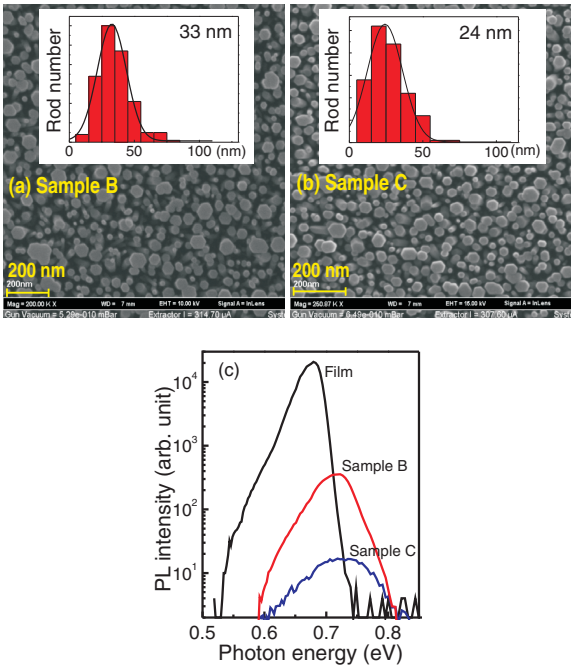

Fig. 1. (a) FE-SEM image of samples B and C with the rod size distribution of each NR film. (b) Semi-logarithmic-scale photoluminescence spectra of an InN epitaxial film and two nanorod samples B and C.

A Ti:sapphire femtosecond laser that delivers ~120 fs optical pulses at 82 MHz repetition rate was employed to excite the samples in the variable-temperature PL spectroscopy. The samples were cooled in a temperature-controlled liquid-He-flow cryostat. The collected luminescence signal was dispersed using a 0.19 m monochromator with a 600 groove/mm grating and detected with a liquid-N_2-cooled extended InGaAs detector (cutoff wavelength ≈2.4 μm). All the PL spectra were corrected with the system response curve.

The morphology and size distribution of InN NRs were analyzed by using field-emission scanning electron microscopy (FE-SEM). The FE-SEM image in Figs. 1(a) and 1(b) indicates that most of the surface area is covered by NRs. The low temperature ($T = 5$ K) PL spectra of the samples B and C as well as the InN epilayer are presented in

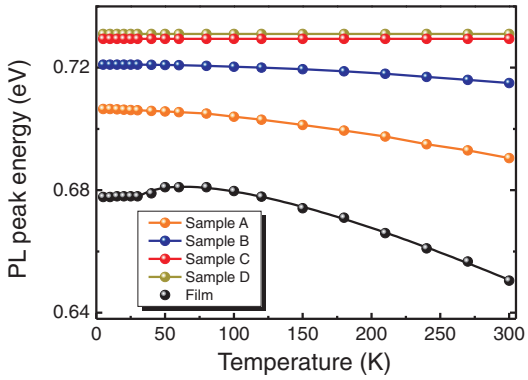

Fig. 2. Temperature-dependent PL peak energy of the InN epitaxial film and the nanorod samples. The temperature dependence of PL peak energy of the epilayer shows a characteristic blueshift at the low temperature range. The solid lines were obtained using Varshni's equation.

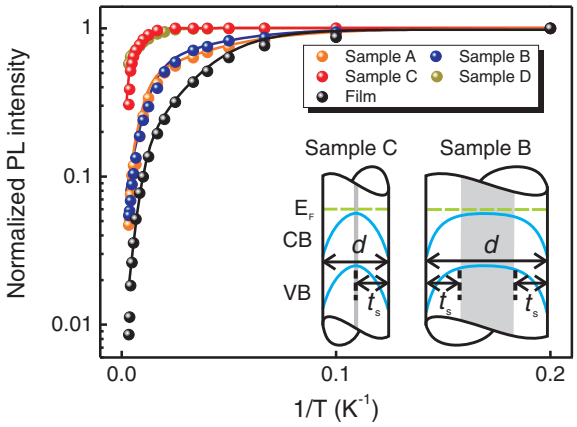

Fig. 3. Intensity variation of the PL intensity as a function of reciprocal temperature for the InN epilayer and the nanorod samples. The activation energies obtained by using Eq. (1) are listed in Table I. Schematics in the figure illustrate the downward surface band bending in samples B and C in an exaggerated scale.

Fig. 1(c). For each measurement, the laser power was kept at 50 mW. The semi-logarithmic PL spectra indicates that the PL efficiencies of the NRs in samples B and C are about two and three orders of magnitude lower than that of the InN epilayer, respectively, which may be due to the smaller effective emission area in the central bulk region of NRs. The full widths at half maximum (FWHM) of the PL spectra of NR samples are much broader than that of the InN epilayer. In contrast to GaN NRs, InN NRs are known to have poorer crystalline quality than the InN epilayer, and the PL spectra from them exhibit a much larger PL band broadening.[9] The PL peak energies for samples B and C locate at 0.72 and 0.73 eV, respectively, while that for the epilayer is ~0.68 eV. The Fermi level shift into the conduction band is known to lead to the increase of the peak energy of PL for *n*-type semiconductors with the increase of electron concentration. A higher peak energy for InN NRs than that for the InN epilayer then indicates that NRs may contain a higher density of free electrons, which are generated during the fabrication of the NRs and occupy states near the bottom of the conduction band. The carrier densities in NRs were separately estimated from the time-domain THz spectroscopy experiment and were found to be about one order of magnitude higher than that of the InN epilayer.[15]

The temperature-dependent PL peak energy of the InN epilayer in Fig. 2 exhibits an *S*-shape dependence and gradually redshifts with a further increase of temperature, following the temperature dependence described by Varshni's equation.[16] The S-shape PL response for the InN film is attributed to the presence of localized states within the tail density of states,[17] and the calculated localization energy for the epilayer sample is ~5.2 meV. The PL spectra of NRs in samples A and B also follow Varshni-like temperature dependence with smaller localization energies than that of the epilayer. In contrast, the PL peak energies of samples C and D are nearly independent of the change in temperature and the dominant influence of the surface accumulation layer was suggested to cause this anomalous PL response.[10]

The most significant size-dependent property of NRs can be found in the temperature-dependent quenching of PL intensity. Figure 3 shows the temperature dependence of the normalized PL intensity (Arrhenius plot) for NR samples, compared with that for the InN epilayer. In the case of the InN epilayer, the PL begins to decrease at as low as 10 K and it drops by at least 2 orders of magnitude at room temperature. PL quenching due to the activation of nonradiative recombination processes can be described by[18]

$$I(T) = \frac{I_0}{1 + C_1 e^{-E_a/k_B T} + C_2 e^{-E_b/k_B T}}, \quad (1)$$

where E_a and E_b are the activation energies at low and high temperatures, respectively, related with the thermal quenching and k_B is the Boltzmann's constant, and C_1 and C_2 are fitting constants. The PL quenching of the InN epilayer is governed by the thermally activated process with $E_a = 4.5$ meV and $E_b = 23$ meV, consistent with the previously reported results.[19]

The thermal quenching process of NRs in Fig. 3 is different from that of the epilayer. The low-temperature/room-temperature PL ratio is significantly smaller in NRs, and the onset temperature of the PL quenching locates at a much higher temperature than that of the epilayer. Particularly for samples C and D, the PL quenching does not occur until ~100 K and the corresponding activation energies listed in Table I are much higher than those of samples A and B.

Larger activation energy implies larger impurity binding energies or carrier/exciton localization energies.[19] As mentioned above, the characteristic S-shape evolution of PL peak energy for the epilayer is attributed to the evolution from localized states to extended band-tail states. Then, the activation energy E_a is related to the delocalization of carriers/excitons and E_b to the quenching from extended states. Meanwhile, larger activation energy of NRs with the shrinkage of NR size implies that the PL processes in NRs may be associated with the carrier redistribution on electronic states within the narrow NRs.[1] Due to Fermi-level pinning at the surface, InN has the downward band bending near the surface and electrons tend to move to the surface, while holes are left in the inner core of NRs. For NRs with $d > 2t_s$, recombination of carriers would occur within the narrow core area, and the PL intensity from these NRs depends on the effective volume of this core area.

Table I. Optical and physical parameters of InN nanorods.

Sample	Rod height (nm)	Rod diameter (nm)	PL peak energy (eV)	E_a (meV)	E_b (meV)
Film	NA	NA	0.678	4.5	23
A	618	143/75	0.706	2.9	26
B	240	33	0.720	5.1	30
C	161	24	0.730	10.0	52
D	146	27	0.731	11.9	63

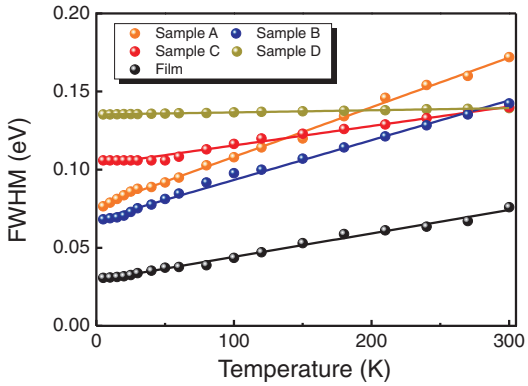

Fig. 4. Temperature-dependent PL bandwidths of the epilayer and the nanorod samples. The temperature dependent broadening is not significant for samples C and D.

Further shrinkage of rod diameter up to $d \approx 2t_s$ leads to the complete depletion of charge within the rod. As the temperature increases, recombination of nonequilibrium carriers in these NRs is reduced or is maybe even impossible if nonradiative recombination via surface traps is the prevailing recombination mechanism. Then, holes in the inner core of NRs can recombine with electrons in the surface accumulation layer only when carriers surpass the band bending energy barrier, V_B, near the surface. Remarkably, the activation energies $E_b = 52$ and 63 meV estimated for samples C and D, respectively, are in excellent agreement with $V_B = 60$ meV known for InN.[20] The delayed fast quenching observed for samples C and D in Fig. 3 then clearly shows the limited carrier recombination in NRs at high temperature.

In Fig. 4, where the temperature dependence of the FWHMs is plotted, the PL spectra of NRs with large diameters (samples A and B) and epilayer become broader linearly with the increase of temperature, whereas the broadening of the PL band is much slower for NRs with the critical diameter (samples C and D). In NRs, holes tend to populate in different sample regions at different values of T, leading to the broadening of the PL bands.[10] Since carrier transportation is limited within the narrow core bulk region of NRs in samples C and D, the PL band broadening may be insignificant at low temperature. Thermalization of carriers at higher temperature then causes the slow broadening of the PL band through the interaction with impurity or defects in the surface layer.

In summary, we have measured temperature-dependent near-infrared PL from InN nanorods. As the nanorod size reduces to a critical value (the thickness of the surface electron accumulation layer), the nonradiative carrier recombination needs a higher activation energy. For InN nanorods with the critical diameter, the activation energy was measured to be consistent with the band bending energy near the surface. We also found that the PL band broadening with the increase of temperature is mainly determined by the core bulk region where the carriers can travel before being captured by surface-associated defects.

Acknowledgments This work was supported by the National Science Council (NSC 101-2112-M-009-012-MY3) and the Science Vanguard Research Program (NSC-101-2628-M-007-006) of Taiwan.

1) C. H. Liang, L. C. Chen, J. S. Hwang, K. H. Chen, Y. T. Hung, and Y. F. Chen: Appl. Phys. Lett. **81** (2002) 22.
2) Z. H. Lan, W. M. Wang, C. L. Sun, S. C. Shi, C. W. Hsu, T. T. Chen, K. H. Chen, C. C. Chen, Y. F. Chen, and L. C. Chen: J. Cryst. Growth **269** (2004) 87.
3) M. C. Johnson, C. J. Lee, E. D. Bourret-Courchesne, S. L. Konsek, S. Aloni, W. Q. Han, and A. Zettl: Appl. Phys. Lett. **85** (2004) 5670.
4) L.-W. Yin, Y. Bando, D. Golberg, and M.-S. Li: Adv. Mater. (Weinheim, Ger.) **16** (2004) 1833.
5) S. Luo, W. Zhou, W. Wang, Z. Zhang, L. Liu, X. Dou, J. Wang, X. Zhao, D. Liu, Y. Gao, L. Song, Y. Xiang, J. Zhou, and S. Xie: Appl. Phys. Lett. **87** (2005) 063109.
6) T. Stoica, R. Meijers, R. Calarco, T. Richter, and H. Lüth: J. Cryst. Growth **290** (2006) 241.
7) H. Ahn, Y.-P. Ku, Y.-C. Wang, C.-H. Chuang, S. Gwo, and C.-L. Pan: Appl. Phys. Lett. **91** (2007) 132108.
8) F. Chen, A. N. Cartwright, H. Lu, and W. J. Schaff: Appl. Phys. Lett. **83** (2003) 4984.
9) H.-Y. Chen, C.-H. Shen, H.-W. Lin, C.-H. Chen, C.-Y. Wu, S. Gwo, V. Yu. Davydov, and A. A. Klochikhin: Thin Solid Films **515** (2006) 961.
10) C.-H. Shen, H.-Y. Chen, H.-W. Lin, S. Gwo, A. A. Klochikhin, and V. Yu. Davydov: Appl. Phys. Lett. **88** (2006) 253104.
11) T. Stoica, R. J. Meijers, R. Calarco, T. Richter, E. Sutter, and H. Lüth: Nano Lett. **6** (2006) 1541.
12) C.-L. Hsiao, H.-C. Hsu, L.-C. Chen, C.-T. Wu, C.-W. Chen, M. Chen, L.-W. Tu, and K.-H. Chen: Appl. Phys. Lett. **91** (2007) 181912.
13) I. Mahboob, T. D. Veal, L. F. J. Piper, C. F. McConville, H. Lu, W. J. Schaff, J. Furthmüller, and F. Bechstedt: Phys. Rev. Lett. **92** (2004) 036804.
14) H. Ahn, C.-C. Yu, P. Yu, J. Tang, Y.-L. Hong, and S. Gwo: Opt. Express **20** (2012) 769.
15) H. Ahn, C.-H. Chuang, Y.-P. Ku, and C.-L. Pan: J. Appl. Phys. **105** (2009) 023707.
16) Y. P. Varshni: Physica **34** (1967) 149.
17) P. G. Eliseev, M. Osinski, J. Lee, T. Sugahara, and S. Sakai: J. Electron. Mater. **29** (2000) 332.
18) E. Monroy, N. Gogneau, F. Enjalbert, F. Fossard, D. Jalabert, E. Bellet-Amalric, L. S. Dang, and B. Daudin: J. Appl. Phys. **94** (2003) 3121.
19) R. Intartaglia, B. Maleyre, S. Ruffenach, O. Briot, T. Taliercio, and B. Gil: Appl. Phys. Lett. **86** (2005) 142104.
20) C.-T. Kuo, S.-C. Lin, K.-K. Chang, H.-W. Shiu, L.-Y. Chang, C.-H. Chen, S.-J. Tang, and S. Gwo: Appl. Phys. Lett. **98** (2011) 052101.